J Therm Anal Calorim (2010) 101:397–402
DOI 10.1007/s10973-009-0513-6

Photopyroelectric calorimetry of solids

FPPE–TWRC method

D. Dadarlat · M. Streza · M. N. Pop · V. Tosa · S. Delenclos · S. Longuemart · A. Hadj Sahraoui

Received: 1 July 2009 / Accepted: 22 September 2009 / Published online: 1 November 2009

Abstract An alternative photopyroelectric (PPE) technique that combines the front detection configuration (FPPE) with the thermal wave resonator cavity (TWRC) method is proposed. The theoretical analysis of the FPPE signal indicates that the configuration also offers information about both fluid sample and backing solid material. It is demonstrated that the normalized phase of the FPPE signal has an oscillating dependence as a function of the sample's thickness. In the thermally thin regime for the sensor and liquid sample, the method can be used for direct measurement of backing thermal effusivity. This article presents experimental results on solid materials, with various values of thermal effusivity (Cu, brass, steel, glass, bakelite, and wood), used as backings in the detection cell. A study of the sensitivity of the technique for different liquid/backing effusivity ratios is performed. The main result of this article is the possibility of deriving the thermal effusivity of a solid sample (backing material) by monitoring the thickness of a fluid with well-known properties. In such a way, the so-called coupling fluid is not anymore a disturbing factor; however, its properties can be used to obtain the value of the thermal effusivity of a solid. The method proved to be suitable especially for thermal effusivity investigations of low thermal conductors. An application on polymer composites with different liquid/powder content is presented.

Keywords PPE technique · Thermal effusivity · Thermal waves · TWRC method

D. Dadarlat · M. Streza (✉) · M. N. Pop · V. Tosa
National R&D Institute for Isotopic and Molecular Technologies, Donath Str. 65-103, CP-400293 Cluj-Napoca, Romania
e-mail: streza.mihaela@gmail.com

S. Delenclos · S. Longuemart · A. H. Sahraoui
Univ Lille Nord de France, CP 59000 Lille, France

S. Delenclos · S. Longuemart · A. H. Sahraoui
ULCO, LDSMM, CP 59140 Dunkerque, France

S. Delenclos · S. Longuemart · A. H. Sahraoui
CNRS UMR8024, CP 59140 Dunkerque, France

Introduction

During the past decades, the photopyroelectric (PPE) calorimetry developed many ways to obtain the values of the thermal parameters of condensed matter samples. Some of the methods are based on the measurement of single values; other alternatives make use of scanning procedures. The second type of investigations is proved to be more precise [1–3].

In principle, one may combine detection configurations (back or front), sources of information (PPE amplitude or phase), and scanning parameters (chopping frequency or sample's thickness), to obtain one dynamic thermal parameter (usually, thermal diffusivity or effusivity) [4–6].

It is well known that, when investigating solid samples, it is not easy to obtain accurate quantitative results, due to the influence of the coupling (sample-sensor) fluid. PPE calorimetry is a contact technique and the coupling fluid, always necessary when investigating solids, leads to uncontrolled errors. This is why, during past years the investigations of thermal properties of solids were more or less avoided.

If we focus our attention on the front photopyroelectric (FPPE) configuration, it was largely used in the past to obtain thermal parameters of liquid and solid samples

[1, 3, 7–9]. In most cases, the FPPE detection cell contained three layers: air, directly irradiated sensor, and (solid or liquid) semi-infinite sample; and the value of the thermal diffusivity and/or effusivity of the sample could be obtained by performing frequency scans of the amplitude or phase of the FPPE signal. Pittois et al. [10] designed for the first time a four-layer FPPE cell, with a thermally thin liquid or solid sample and a semi-infinite backing material. With a restriction of "very good thermal conductor backing," they could derive both thermal conductivity and effusivity of the sample, by performing a frequency scan of the PPE signal over a large frequency range.

On the contrary, Mandelis and co-workers [1, 11, 12] proposed, during the past decade, the so-called thermal wave resonator cavity (TWRC) method as an alternative to frequency scanning procedures. The method, in the back detection configuration, showed to be suitable and very accurate for investigating thermal properties (especially thermal diffusivity) of liquids [7, 9, 13, 14].

In this work, we propose an alternative technique that combines the FPPE configuration with the TWRC method; in this configuration, by monitoring the thickness of a fluid sample, the thermal effusivity of a solid material used as backing in the detection cell can be measured. In such a way, the coupling fluid is not anymore a disturbing factor, but its properties can be used to obtain the value of the thermal effusivity of a solid.

Theoretical aspects

In the FPPE configuration, the radiation impinges on the front surface of the pyroelectric sensor, and the sample, in good thermal contact with its rear side, acts as a heat sink. The detection layout (Fig. 1) is practically the same as proposed in [10], but without any restriction concerning the thermal properties of the backing material.

In the approximation of the one-directional heat propagation and thermally thin limit for the sensor ($\exp(\pm\sigma_p L_p) = 1 \pm \sigma_p L_p$), the normalized complex PPE signal is given by [4, 5, 15]

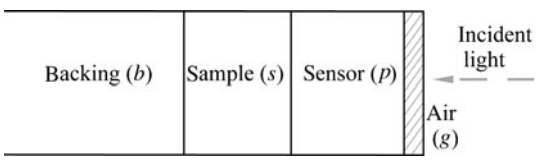

Fig. 1 Layout of the detection cell for a FPPE–TWRC configuration

$$V = \frac{[S(b_{bs}+1) - S^{-1}(b_{bs}-1)](\sigma_p L_p)}{(\sigma_p L_p)[S(b_{bs}+1) - S^{-1}(b_{bs}-1)] + b_{sp}[S(b_{bs}+1) + S^{-1}(b_{bs}-1)]}, \quad (1)$$

where

$$S = \exp(\sigma_s L_s),\ \sigma_j = (1+i)a_j;\ \mu = (2\alpha/\omega)^{1/2}, b_{ij} = e_i/e_j \quad (2)$$

In Eqs. 1 and 2, ω is the angular chopping frequency of radiation, σ and a are the complex thermal diffusion coefficient and the reciprocal of the thermal diffusion length ($a = 1/\mu$), respectively. Symbols "p," "s," and "b" refer to pyroelectric sensor, liquid sample (acting as a coupling fluid in our case), and backing material, respectively. The normalization of Eq. 1 was performed with the signal obtained with the sensor standing alone in air (i.e. no sample and air as a backing).

In order to compare results obtained with different liquid samples and backing materials, it is useful to perform a second normalization with the signal obtained with very thick liquid sample ($\exp(-\sigma_s L_s) = 0$). The result is given by:

$$V_n = \frac{\sigma_p L_p + b_{sp}}{(\sigma_p L_p) + b_{sp}\left[\frac{1+R_{bs}\exp(-2\sigma_s L_s)}{1-R_{bs}\exp(-2\sigma_s L_s)}\right]}, \quad (3)$$

where $R_{ij} = (b_{ij} - 1)/(b_{ij} + 1)$ represents the reflection coefficient of the thermal wave at the "ij" interface.

The normalized PPE signal (Eq. 3) depends on the thermal effusivity of the backing material; a thickness scan of the amplitude and/or phase of the PPE signal (at constant chopping frequency) will lead to its direct measurement.

In the following section, we will focus our attention on the phase of the PPE signal. It is more convenient to obtain information from the phase of the signal, because the phase does not depend on the fluctuations of the incident power and/or the quality of incident surface. A mathematical simulation of the normalized phase of the PPE signal (Eq. 3), for different e_b/e_s ratios, is presented in Fig. 2.

Figure 2 indicates that the normalized phase of the PPE signal has an oscillating value as a function of the thickness of the liquid sample. For large sample thicknesses, the normalized phase becomes zero but, in the thermally thin regime for the sample, the phase seems to be sensitive to the thermal effusivity of the backing material. We can identify some "zero-crossing points" in Fig. 2 given by the following transcendental equation:

$$\left(1 + \frac{b_{sp}}{y}\right)\sin(2x) + \cos(2x) = R_{bs}\exp(-2x), \quad (4)$$

where $y = L_p/\mu_p$ and $x = L_s/\mu_s$.

If we restrict our attention to the first zero-crossing point, from theoretical point of view, it is almost independent on R_{bs}, due to the very quick decrease of the

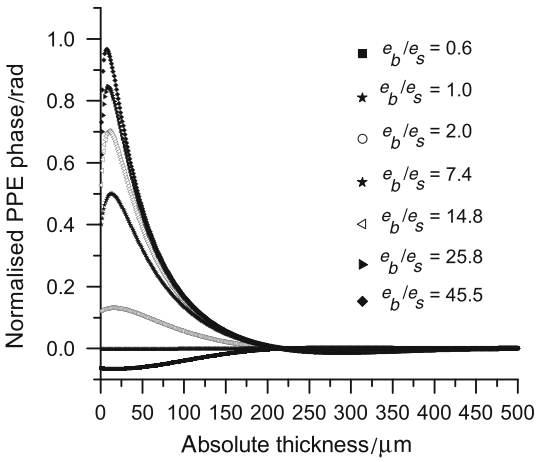

Fig. 2 Mathematical simulation of the normalized phase of the PPE signal (Eq. 3), for different e_b/e_s ratios, ranging from 0.6 to 45.5

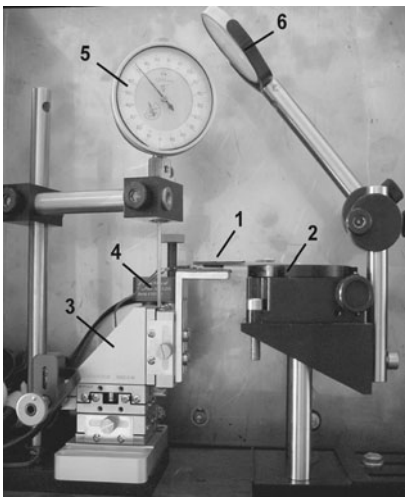

Fig. 3 Image of the back detection cell presently used by the authors: 1—sensor-sample assembly; 2—rotating table; 3—XYZ motion control system; 4—motor with nanometer resolution for vertical motion control; 5—micrometer; 6—mirror reflecting the incident laser radiation

amplitude of the oscillations of the normalized phase with increasing thickness [15]. As a consequence one can obtain, from the x-value of the zero-crossing point, sample's thermal diffusivity. However, due to the shape of the curve "PPE phase versus sample's thickness," the zero-crossing points are difficult to be obtained with enough precision. From experimental point of view, it is more convenient and more precise to perform a fit on the experimental points, in the thermally thin regime for the sample, with the sample's absolute thickness and backing's thermal effusivity as fitting parameters.

Experimental setup

The experimental setup is classical for FPPE calorimetry, and it was mostly described before [6, 9, 15]. Only some details will be presented here.

The pyroelectric sensor, a 100-μm thick $LiTaO_3$ single crystal ($e_p = 3.66 \times 10^3$ $Ws^{1/2}$ m^{-2} K^{-1}; $\alpha_p = 1.36 \times 10^{-6}$ m^2 s^{-1}), provided with Cr-Au electrodes on both faces, is glued on a rotating stage. The backing material is situated on a micrometric stage. The modulated radiation (30 mW HeNe laser) is partially absorbed by the front electrode of the sensor. The space between the sensor and the backing material accommodates the liquid sample. The sample's thickness variation is performed with a step of 0.03 μm (9062M-XYZ-PPP Gothic-Arch-Bearing Picomotor), and the data acquisition was taken each 30th step. The "rough" control of the sample's thickness and the parallelism between backing and sensor are assured by 3- and 6-axis micrometric stages. During the scanning procedure, the sample's thickness variation is very rigorously controlled, but the absolute sample's thickness is not precisely known. Its correct value is obtained, as explained in the theoretical section, only as a result of a fitting procedure. An image of the front detection cell currently used by the authors is shown in Fig. 3.

All the measurements were performed at room temperature. The PPE signal was processed with a SR 830 lock-in amplifier. The data acquisition, processing, and analysis were performed with adequate software.

Two liquid samples, water ($e_s = 16.0 \times 10^2$ $Ws^{1/2}$ m^{-2} K^{-1}; $\alpha_s = 14.6 \times 10^{-8}$ m^2 s^{-1}) and ethylene glycol ($e_s = 8.14 \times 10^2$ $Ws^{1/2}$ m^{-2} K^{-1}; $\alpha_s = 9.36 \times 10^{-8}$ m^2 s^{-1}), and several backing solids with different values of thermal effusivity (wood (oak), bakelite, glass, steel, brass, and Cu) were selected for investigations.

Results and discussions

Typical behaviors of the normalized phase of the FPPE signal, for a detection cell with ethylene glycol as liquid sample and different solids as backing materials (wood, bakelite, glass, and Cu), together with the results obtained for the thermal effusivity, are shown in Fig. 4 and Table 1. As mentioned before, the value of the thermal effusivity was obtained by optimizing the fit performed with Eq. 1, on the experimental points from the thermally thin region for the sample, with sample's absolute thickness and backing's thermal effusivity as fit parameters.

Figure 4 indicates that the values of the thermal effusivity obtained for oak, bakelite, and glass are in good agreement with the literature data [16]. Concerning the thermal effusivity obtained for Cu, its value is about 50%

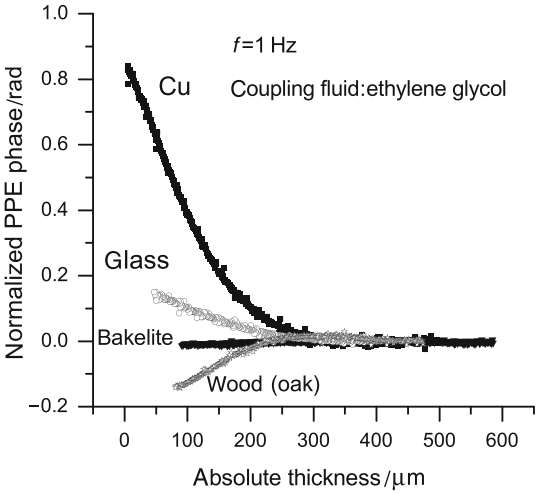

Fig. 4 Normalized phase of the FPPE signal as a function of sample's absolute thickness, for a detection cell with ethylene glycol as liquid sample and different solids as backing materials (wood, bakelite, glass, Cu)

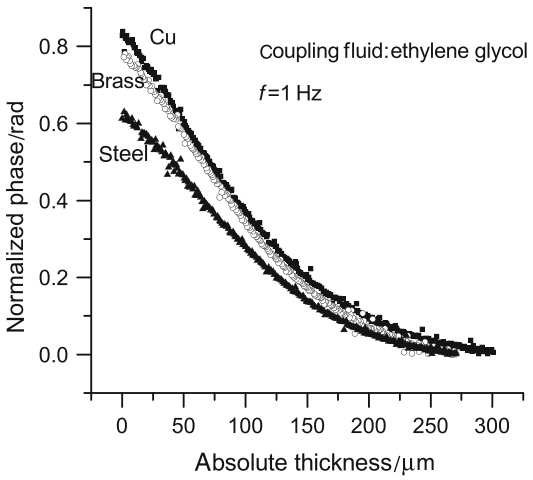

Fig. 5 Same as Fig. 4, but only for metallic backings (Cu, brass, and steel)

lower than the literature data. Results obtained for other metals, and shown in Fig. 5, indicate that the value of the thermal effusivity, obtained by our method, agrees better with previously reported values if the thermal effusivities of the backing and liquid sample are close.

Table 1 presents the values of the thermal effusivity obtained by our method for several solid materials, together with the literature data [16–19].

If we used water as liquid sample instead of ethylene glycol, we found reproducible values for the thermal effusivity within about 5–7% relative error (see Fig. 6 for bakelite).

Figure 7 presents the results obtained on a dental filling material (polymer composite), specially selected for its thermal effusivity situated somewhere between the thermal effusivities of water and ethylene glycol.

The discrepancies (as compared with literature data) obtained for the values of the thermal effusivity of good thermal conductors oblige us to perform a study of the accuracy of the fits as a function of e_b/e_s.

Table 1 The value of thermal effusivity for some solid materials, as obtained by FPPE–TWRC technique, compared with literature data [16, 18, 19]

Material	Thermal effusivity/ $Ws^{1/2}\ m^{-2}\ K^{-1}$ (FPPE–TWRC)	Thermal effusivity/ $Ws^{1/2}\ m^{-2}\ K^{-1}$ (literature)
Cu	18300	37136 [16]
Brass	12850	13863 [16]–17980 [18]
Steel	6350	6090 [19]–7187 [16]
Glass	1300	1275 [18, 19]–1600 [16]
Bakelite	750	681 [16]
Wood	350	122 [18]–470 [16]

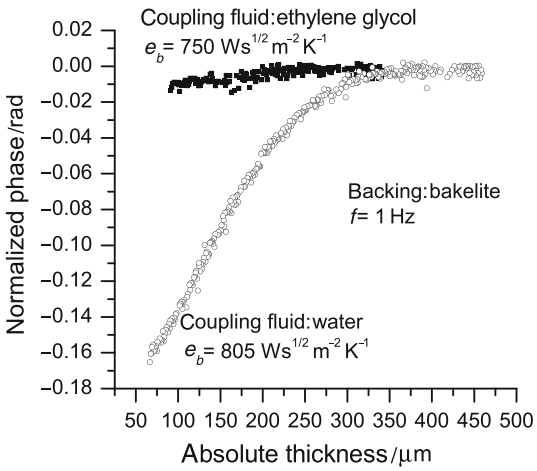

Fig. 6 Normalized phase of the FPPE signal as a function of sample's absolute thickness, for a detection cell with bakelite as backing material and two different coupling fluids ethylene glycol and water

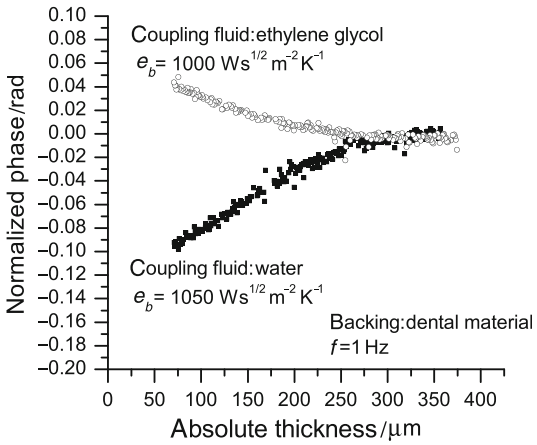

Fig. 7 Same as Fig. 6, but with a polymer composite as backing material

Figures 8 and 9 represent contour maps of the precision of the fits for two materials: Cu, with large e_b/e_s, ($\approx$45) and glass with e_b/e_s close to one ($\approx$1.6)

The contour map from Fig. 8 indicates that, in the case of large e_b/e_s, the exact measurement of the sample's absolute thickness is rather precise, but the dependence of the "chi-squared" of the fit as a function of backing's thermal effusivity has a large minimum.

When $e_b \approx e_s$ (Fig. 9), the exact location of the backing position is more difficult, but the measured value of the backing's thermal effusivity is more precise.

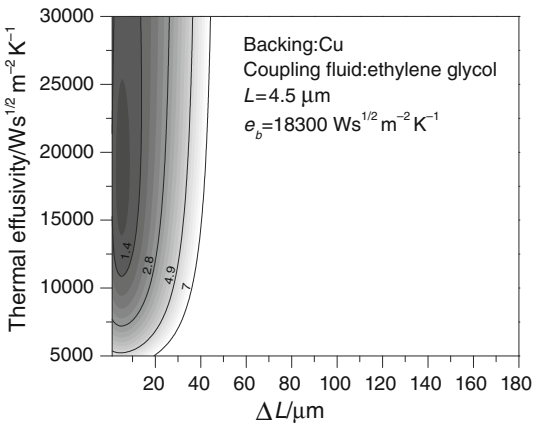

Fig. 8 Contour map of the precision of the fit performed with Eq. 1 on the experimental data obtained on Cu backing. *X*-axis represents the correction term in the measurement of the absolute liquid's thickness. The shape of the contour curves indicates a good localization of the position of the backing, but lower precision in the value of thermal effusivity

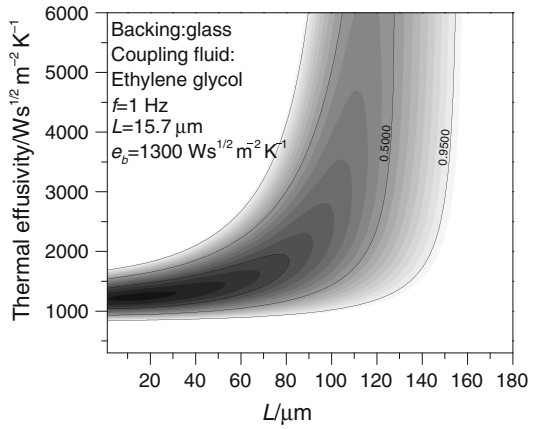

Fig. 9 Contour map of the precision of the fit performed with Eq. 1 on the experimental data obtained on glass backing. *X*-axis represents the correction term in the measurement of the absolute liquid's thickness. The shape of the contour curves indicates a bad localization of the position of the backing, but good precision in the value of thermal effusivity

At the end of this section, we want to support the suitability of this configuration in thermal effusivity investigations on solids by performing some measurements on some conventional and modified glass-ionomers cements. The selection of this type of solid materials was imposed by the recent increasing interest in their thermal biocompatibility (similar values of thermal parameters with human teeth), but, in the framework of our paper, mainly by the value of their thermal effusivity, which is close to the thermal effusivity of ethylene glycol (see Fig. 7).

The preparation of the glass-ionomers cements was described before [17, 20]. The samples were prepared at 23 °C from the aqueous solutions of the copolymers (polyalkenoic acids) and the superficially active glasses, by spatulating the powders and liquids on a glass slab. The samples, having the form of disks of 6 mm diameter and 0.4 mm height, were obtained by hardening of freshly mixed pastes in Teflon molds, which were hermetically closed and stored in water at 37 °C. After about 30 min, the disks were taken out of molds and were immediately immersed in water at 37 °C, for 24 h. The hardening of the photopolymerizable resin-modified glass-ionomer composite was accomplished by mixing the powder with the proper liquid at the desired ratio and by exposing the obtained pastes to a visible radiation (400–500 nm) for 180 s.

The results are shown in Fig. 10, together with the results obtained in Ref. [17], for the values of thermal diffusivity.

The trend of the variation of thermal diffusivity as a function of powder/liquid ratio, observed for the investigated polymers, is in good agreement with our results.

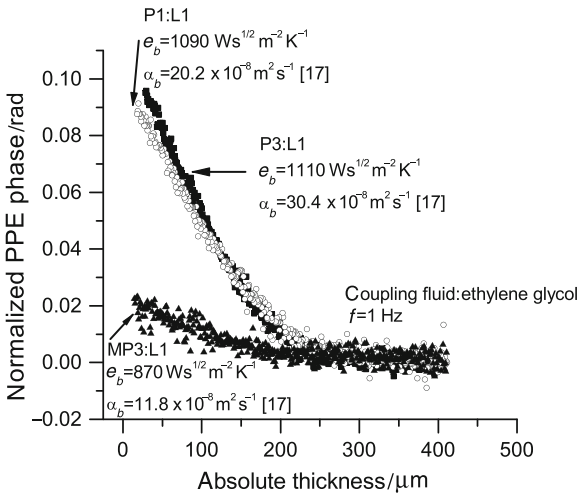

Fig. 10 Normalized phase of the FPPE signal as a function of sample's absolute thickness, for a detection cell with ethylene glycol as liquid sample and different dental polymers as backing materials. P:L indicates the powder:liquid ratio [17]. Symbol M indicates a modified polymer [17, 20]

Conclusions

The FPPE together with the TWRC method was used for direct measurement of the thermal effusivity of solid materials inserted as backings in the FPPE detection cell. The experimental results obtained on solid materials with various values of thermal effusivity show that the highest sensitivity was obtained when investigating solids with values of thermal effusivity close to the effusivity of the liquid layer of the detection cell. In such cases, the typical relative errors are of about $\pm 2.5\%$, comparable or better than those obtained by typical frequency scanning procedures. In any case, by using this method, the uncertainty in the thickness of the thin layer of coupling fluid used in the typical frequency scanning procedures is eliminated. In conclusion, the method seems to be suitable for measuring thermal effusivity of low thermal conductors. An application performed on some dental cements of last generation supports the validity of this remark.

Acknowledgements Work supported in part by the Romanian Ministry of Education and Research through the National Research Programs PN09 44 02 03 and PN II 372 and by bilateral (NIRDIMT Cluj- Univ. Littoral Dunkerque) Brancusi Project. The authors acknowledge the support from Drs. C. Prejmerean and L. Silaghi-Dumitrescu for the preparation of dental filling materials.

References

1. Mandelis A, Matvienko A. Photopyroelectric thermal-wave cavity devices-10 years later. In: Remiens Denis, editor. Pyroelectric materials and sensors. Kerala, India: Research Signpost; 2007. p. 61–96.
2. Delenclos S, Dadarlat D, Houriez N, Longuemart S, Kolinsky C, Hadj Sahraoui A. On the accurate determination of thermal diffusivity of liquids by using the photopyroelectric thickness scanning method. Rev Sci Instrum. 2007;78:024902.
3. Dadarlat D, Neamtu C, Pop R, Marinelli M, Mercuri F. On the selection of the experimental parameters in a thermal-wave-resonator-cavity (TWRC) configuration. J Optoelectron Adv Mat. 2007;9:2847–52.
4. Mandelis A, Zver MM. Theory of the photopyroelectric effect in solids. J Appl Phys. 1985;57:4421–30.
5. Chirtoc M, Mihailescu G. Theory of the photopyroelectric method for investigation of optical and thermal materials properties. Phys Rev. 1989;B40:9606–17.
6. Dadarlat D, Bicanic D, Visser H, Mercuri F, Frandas A. Photopyroelectric method for determination of thermophysical parameters and detection of phase transitions in fatty acids and triglycerides. Part I: principles, theory and instrumentational concepts. J Am Oil Chem Soc. 1995;72:273–8.
7. Dadarlat D, Chirtoc M, Neamtu C, Candea R, Bicanic D. Inverse photopyroelectric detection method. Phys Stat Sol. 1990; 121:K231–34.
8. Dadarlat D, Neamtu C. Detection of molecular associations in liquids by photopyroelectric measurements of thermal effusivity. Meas Sci Technol. 2006;17:3250–4.
9. Dadarlat D, Neamtu C. High performance photopyroelectric calorimetry of liquids. Acta Chim Slovenica. 2009;56:225–36.
10. Pittois S, Chirtoc M, Glorieux C, Bril W, Van den Thoen J. Direct determination of thermal conductivity of solids and liquids at very low frequencies using the photopyroelectric method. Anal Sci. 2001;17:S110–3.
11. Shen J, Mandelis A. Thermal-wave resonator cavity. Rev Sci Instrum. 1995;66:4999–5005.
12. Shen J, Mandelis A, Tsai H. Signal generation mechanism, intercavity-gas thermal diffusivity temperature dependence and absolute infrared emissivity measurements in a thermal-wave resonant cavity. Rev Sci Instrum. 1998;69:197–203.
13. Balderas-Lopez LA, Mandelis A, Garcia JA. Thermal-wave resonator cavity design and measurements of the thermal diffusivity of liquids. Rev Sci Instrum. 2000;71:2933–7.
14. Balderas-Lopez LA, Mandelis. Self-consistent photothermal techniques: application for measuring termal diffusivity in vegetable oils. A Rev Sci Instrum. 2003;74:700–2.
15. Streza M, Pop MN, Kovacs K, Simon V, Longuemart S, Dadarlat D. Thermal effusivity investigations of solid materials by using the thermal-wave-resonator-cavity (TWRC) configuration. Theory and mathematical simulations. Laser Phys. 2000;19:1340–4.
16. Mandelis A. Principles and perspectives of photothermal and photoacoustic phenomena. New York: Elsevier; 1992.
17. Streza M, Dadarlat D, Simon V, Prejmerean C, Silaghi-Dumitrescu L. Thermal diffusivity investigations of some dental materials by using photopyroelectric calorimetry. J Optoelectron Adv Mat- Symposia. 2009;1:70–3.
18. Perry JH. Chemical engineering handbook. New York: McGraw-Hill; 1963.
19. Touloukian YS. Thermophysical properties of high temperatures solid materials. New York: MacMillan; 1967.
20. Prejmerean C, Tomoaia GH, Tomoaia-Cotisel M, Mocanu A, Horovitz O, Moldovan M, et al. Surface organization and stability of some composites exposed to biologic medium. Atomic force microscopy observations. J Optoelectron Adv Mat. 2008;10:597–601.